Proceedings of the 9th U.S. National and 10th Canadian Conference on Earthquake Engineering
Compte Rendu de la 9ième Conférence Nationale Américaine et
10ième Conférence Canadienne de Génie Parasismique
July 25-29, 2010, Toronto, Ontario, Canada • Paper No 1074

DEVELOPMENT OF A LARGE-SCALE MR DAMPER MODEL FOR SEISMIC HAZARD MITIGATION ASSESSMENT OF STRUCTURES

Yunbyeong Chae[1], James M. Ricles[2] and Richard Sause[3]

ABSTRACT

During the past decade a number of researchers have investigated the behavior of magneto-rheological (MR) dampers and semi-active control laws associated with using these devices for earthquake hazard mitigation of civil engineering structural systems. A majority of this research has involved reduced-scale MR dampers. A new MR damper model is developed based on full-scale damper characterization tests. The new MR damper model can independently describe the pre-yield and post-yield behavior of an MR damper, simplifying the process to identify the parameters for the model. The model utilizes the Hershel-Bulkley visco-plasticity to describe the post-yield behavior with shear thinning and thickening of the MR fluid. A nonlinear differential equation is proposed to describe the dynamics of an MR damper associated with variable current input. The accuracy of the new MR damper model is compared with existing MR damper models and experimental tests results. The comparisons show that the new model can achieve better accuracy in predicting damper behavior.

Introduction

Magneto-rheological (MR) dampers are devices which can have their characteristics vary by changing the input current to the damper. The MR damper force depends on the yield stress of the MR fluid inside the damper, which is a function of the input current to the damper. When an MR fluid is subjected to a magnetic field, the iron particles in the fluid are aligned and form linear chains parallel to the field, changing the state of the fluid to a semi-solid, which in turn increases the fluid viscosity and restricts the fluid movement through the orifices in an MR damper. This results in changing the yield stress of the MR fluid. MR dampers can be used for seismic hazard mitigation by incorporating these devices into structures. Dyke et al. (1996) studied the feasibility of an MR damper as a means of suppressing vibrations in a structure using a clipped optimal controller algorithm. Thereafter, numerous researchers have studied the behavior of structures with passively or semi-actively controlled MR dampers (Janson and Dyke 2000, Schurter and Roschke 2001, Ribakov and Gluck 2002). Most of those studies involved small-scale MR dampers, which may not be applicable to real structures.

[1] Graduate Research Assistant, Dept. of Civil & Env. Eng., Lehigh University, Bethlehem, PA 18015
[2] Bruce G. Johnston Professor, Dept. of Civil & Env. Eng., Lehigh University, Bethlehem, PA 18015
[3] Joseph T. Stuart Professor, Dept. of Civil & Env. Eng., Lehigh University, Bethlehem, PA 18015

Large-scale MR dampers have been experimentally investigated by numerous researchers (Carlson and Spencer 1996, Yang 2001, Sodeyama et al. 2004, Bass and Christenson 2007). Numerous damper models have been developed to predict the behavior of MR dampers (Spencer et al. 1997, Butz and Von Stryk 2002, and Gavin 2001). Among those models, the Bouc-Wen model (Spencer et al. 1997) and hyperbolic tangent model (Gavin 2001) are popular, and have been used by Yang et al. (2002) and Bass and Christenson (2007) to model large-scale MR dampers. Both the Bouc-Wen model and the hyperbolic tangent model can accurately predict the frequency dependent behavior and roll-off phenomenon that occurs at low velocities in MR dampers. However, due to the complexity of these nonlinear models the estimation of the model parameters can be difficult. Moreover, it is difficult for these models to accurately describe the shear thinning or thickening behavior that occurs in the MR fluid (Yang 2001) during the post yield response when high velocities can develop in the damper. In both the Bouc-Wen and hyperbolic tangent models the post-yield behavior is predominantly described by a linear dashpot; hence, the post-yield behavior of these models is a Newtonian fluid motion where the damper force is proportional to velocity. This can result in an inaccurate prediction of damper force at large amplitudes and high velocities, where under these conditions a non-Newtonian fluid behavior is experimentally observed to occur in the MR fluid.

This paper describes called the newly developed *Maxwell Nonlinear Slider* (MNS) model for modeling large-scale MR dampers. Characterization tests are conducted on a large-scale damper to identify the parameters for the MNS model. Comparisons are subsequently made between the behavior predicted by the MNS model and that measured while subjecting large-scale dampers to varying displacement and current histories. The results are shown to have better accuracy than existing models when applied toward the modeling of large-scale MR dampers.

Maxwell Nonlinear Slider MR Damper Model

The components of the MNS model are shown in Fig. 1. The model has two modes: pre-yield and post-yield. In Fig. 1, x is a degree of freedom of the model that is associated with the deformation of the damper, while y and z are variables associated with the pre-yield mode of the model. One of the advantages of the MNS model is that the pre- and post-yield modes of response can be separated from each other, enabling the model parameters that describe these two modes of behavior to be independently identified. This makes it easier to identify the parameters for the model compared to other existing MR damper models.

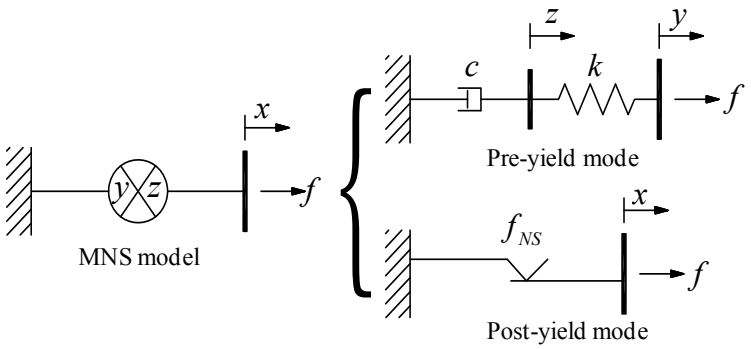

Figure 1. Proposed phenomenological MR damper model: Maxwell Nonlinear Slider (MNS) MR damper model

Pre-Yield Mode

During the pre-yield mode, the behavior of the damper is described by a Maxwell element, hence, the damper force *f* is determined by solving the following differential equation

$$f = k(y - z) = c\dot{z} \tag{1}$$

When the damper is in pre-yield mode, $\dot{y}$ is equal to the damper velocity $\dot{x}$. The initial value of y is set to be equal to x; thus Eq. 1 can be solved in terms of z for a given x and the damper force is then determined. The values of c and k for the Maxwell element are obtained from the force-velocity relationship observed in damper characterization tests, selecting two appropriate points on the hysteretic response curve and then applying visco-elasticity theory. Assuming the Maxwell element is subjected to a harmonic motion with an amplitude of u_0 and circular excitation frequency of ω, the coefficients c and k are calculated as follows:

$$c = \frac{1}{u_0\omega}\frac{f_0^2 + f_m^2}{f_m}, \qquad k = \frac{1}{u_0}\frac{f_0^2 + f_m^2}{f_0} \tag{2}$$

where f_0 and f_m are the damper force when the damper velocity is zero and a maximum value, respectively.

Post-Yield Mode

The post-yield behavior of the MNS model is described by the nonlinear slider which a frictional force defined by a set of post-yield curves that are pre-defined trajectories of the damper force on the force-velocity plane. In the post-yield mode the force is based on considering the velocity at the degree of freedom x, i.e., $\dot{x}$. Fig. 2 shows the post-yield curves for the MNS model, where a curve is defined for both the positive and negative force and referred to as the *positive* and *negative force post-yield curves*, respectively. Each post-yield curve is based on the Herschel-Bulkley model (Herschel and Bulkley 1926) and a linear line that is tangential to this curve at the velocity of $\dot{x}_t^+$ or $\dot{x}_t^-$ as shown in Fig. 2. Since the Herschel-Bulkley model is incorporated into the MNS model, the property of a non-Newtonian fluid can be easily described by the MNS model. The mathematical representation of the positive force post-yield curve for the MNS model is given by

$$f_{py}^+(\dot{x}) = \begin{cases} a + b|\dot{x}|^n & \text{if } \dot{x} \geq \dot{x}_t^+ \\ a_t(\dot{x} - \dot{x}_t^+) + f_t^+ & \text{if } \dot{x} < \dot{x}_t^+ \end{cases} \tag{3}$$

where a, b, n, and $\dot{x}_t^+$ are parameters to be identified from damper characterization tests; and $a_t = bn|\dot{x}_t^+|^{n-1} a_t = bn|\dot{x}_t^+|^{n-1}$ and $f_t^+ = a + b|\dot{x}_t^+|^n$. The negative force post-yield curve, $f_{py}^-(\dot{x})$, can be defined in a similar manner as $f_{py}^+(\dot{x})$ using the appropriate values for the negative force post-yield curve parameters. The simplicity of the Herschel-Bulkley model enables values for the model parameters to be readily obtained from characterization tests since the post-yield behavior is independent of the identification of the Maxwell element parameters *c* and *k* that describe the pre-yield mode of the MNS model.

The post-yield curve of Eq. 3 is dependent only on the velocity $\dot{x}$. However, data from damper characterization tests performed by the authors show a slight discrepancy between the force predicted by the model and that measured in the damper when the velocity $\dot{x}$ and acceleration $\ddot{x}$ of the damper motion are in opposite directions during the post-yield mode of behavior. To account for this behavior, an inertial term is added to the post-yield damper force for the MNS model, whereby the force f in the damper is:

$$f = \begin{cases} f_{py}(\dot{x}) & \text{if } \dot{x} \cdot \ddot{x} \geq 0 \\ f_{py}(\dot{x}) + m_0 \ddot{x} & \text{otherwise} \end{cases} \tag{4}$$

In Eq. 4 f_{py} is either the positive or negative force post-yield curve and m_0 is a mass to account for the force discrepancy. The value for the parameter m_0 can be obtained by equating the product of the measured acceleration and m_0 to the discrepancy between the post-yield mode measured damper force and the predicted force by the MNS model without the inertia term, where the measured quantities are from damper characterization tests.

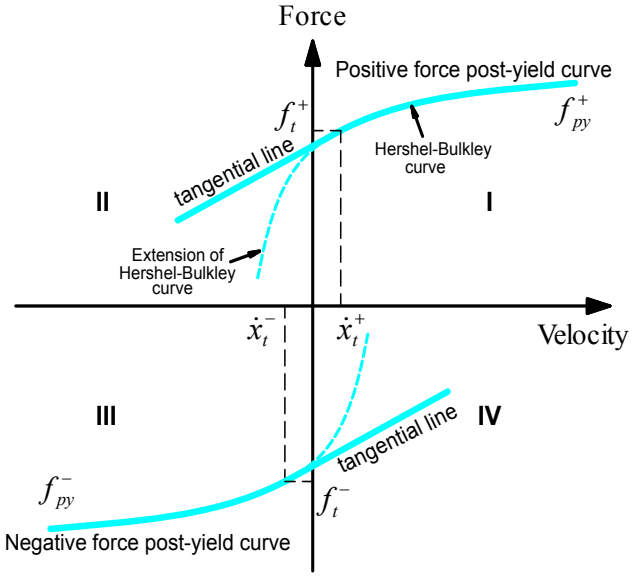

Figure 2. Pre-defined post-yield curves for MNS model

Criteria for Mode Change

When the damper force f from the Maxwell element reaches the post-yield curve, the nonlinear slider is activated and the mode changes from the pre-yield to the post-yield state. Mathematically, this condition is expressed as

$$|f| = |f_{py}(\dot{x})| \tag{5}$$

Eq. 5 implies that the generated damper force is always bounded by the positive and negative force post-yield curves in the MNS model. The transition from the post-yield mode to the pre-yield mode occurs when the following velocity equation is satisfied during the post-yield mode

$$\dot{x} = \dot{y} \tag{6}$$

where, $\dot{y}$ is calculated from

$$\dot{y} = \frac{\dot{f}}{k} + \frac{f}{c} \tag{7}$$

Eq. 7 is obtained by solving for y from Eq. (1) and then taking the time derivative of y. The value for $\dot{y}$ is then calculated by substituting the damper force f and the time derivative of the damper force, $\dot{f}$, from the post-yield mode into Eq. 7. To obtain a smooth transition from the post-yield mode to the pre-yield mode, during the post-yield mode of behavior the pre-yield mode variables y and z of the model are continuously updated by solving Eq. (1) for z and then y using the force f developed in the damper during post-yield mode.

Damper Characterization Tests

Characterization tests were performed at the Lehigh NEES equipment site on a large-scale MR damper. The damper is manufactured by Lord Corporation and is similar to the MR dampers used by Bass and Christenson in their research. The damper is shown schematically in Fig. 3(a). The length and available stroke of the damper are 1.5m and ±290mm, respectively. The electromagnetic coil consists of 368 turns of 18 AWG magnet wire with an annular gap of 1.0 mm between the piston head and the inside diameter of the cylinder. The damper is filled with approximately 19 liters of MRF-132DG type MR fluid manufactured by Lord Corporation.

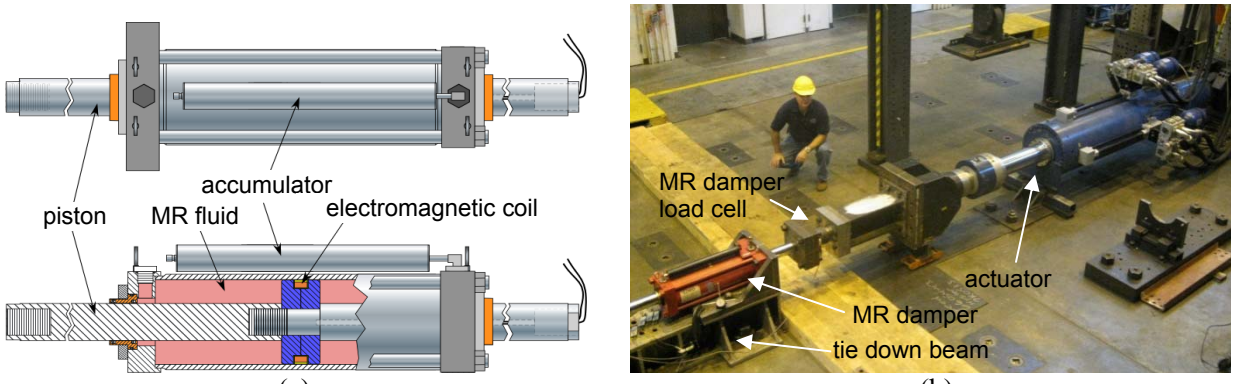

(a) (b)

Figure 3. (a) Schematic of a large-scale MR damper by Lord Corporation (after Bass and Christenson 2007); (b) experimental setup for the characterization test of MR damper

The experimental setup for the characterization test consists of primary two parts: i) a hydraulic actuator to control the movement of the MR damper; and ii) electrical hardware to supply an appropriate current to the damper for the control of the damper force. Fig. 3(b) shows the test setup for the characterization test of the MR damper. The MR damper is connected to the hydraulic actuator through a stiff horizontal steel section. This is done in order to extend the arm of the actuator piston to accommodate the spacing of anchor locations for threaded rods that secure the damper and actuator to the laboratory strong floor. The maximum force capacity of

the actuator is 1,700kN; with the actuator having the ability to generate approximately 500kN of force at a piston velocity of 1.0m/sec. A 534kN load cell is installed between the horizontal steel section and the damper piston to directly measure the force developed in the damper.

The current going into the damper is controlled by a pulse width modulation (PWM) type current driver manufactured by Advanced Motion Controls (30A8). The PWM servo-amplifier can supply the current to the electrical circuit up to 30A by driving the DC motor at a high rate of switching frequency (22kHz). To reduce the noise from the electrical power source, a Schaffner line filter is deployed in front of the DC power supply that provides 72 DC voltage to the PWM servo-amplifier. The command current is transferred to the PWM servo-amplifier through voltage signals from -10V to +10V to produce the desired current utilizing pulse width modulation. The current going into the MR damper is monitored by a current probe (CR Magnetics current transformer).

Table 1. Identified parameters for MNS damper model

Current, I (Amps)	c (kN s/m)	k (kN/m)	Positve force post-yield curve				Negative force post-yield curve				m_0 (kN s^2/m)
			a (kN)	b (kN s/m)	n	$\dot{x}_t^+$ (m/s)	a (kN)	b (kN s/m)	n	$\dot{x}_t^-$ (m/s)	
0.0	10,000	100,000	7.5	243.5	1.62	0.010	-7.3	-235.6	1.60	-0.010	0.50
0.5	11,000	100,000	53.1	162.5	0.85	0.010	-53.1	-162.5	0.85	-0.010	0.50
1.0	12,000	118,000	91.5	122.5	0.52	0.010	-96.0	-134.9	0.60	-0.010	1.60
1.5	12,000	118,000	126.7	152.1	0.58	0.010	-126.7	-152.1	0.58	-0.010	1.50
2.0	11,491	110,030	148.5	166.3	0.66	0.003	-146.8	-182.1	0.71	-0.003	1.05
2.5	12,278	112,890	138.5	161.8	0.46	0.017	-133.5	-171.8	0.46	-0.012	1.04

The parameters for the MNS damper model are identified in such a manner that a minimal error is achieved between the damper force predicted by the model and that measured during the characterization tests. In this paper the particle swarm optimization (PSO) algorithm by Kennedy and Eberhart (1995) is used for the identification of the damper model parameters. The normalized root mean square (RMS) error by Gavin (2001) is used as the objective function that is minimized to establish the values of the model parameters. The parameters are obtained for a range of selected currents from various characterization tests involving sinusoidal displacement histories. For each current level, four different sinusoidal tests with the amplitude of 25.4mm and frequencies of 0.5Hz, 1.0Hz, 2.0Hz, and 3.0Hz were conducted for the identification of the model parameters. Table 1 shows the identified parameters of the MNS model for the various current levels. To compare the performance of the MNS model with the Bouc-Wen and hyperbolic tangent models the parameters for these other models are also identified using the PSO applied to the same experimental data set, where in the PSO the number of particles and iterations was assigned to assure the convergence of the model parameters.

Experimental Evaluation of MNS Model under Constant Current

The MNS model was evaluated by comparing the damper response predicted by the model with that recorded in tests where the displacement history was based on selected Gaussian white noise (see Fig. 4(a) and Table 2). The comparisons are shown in Fig. 4(b), (c) and (d), where the damper force time history, damper force-displacement, and damper force-velocity are

given, respectively. The current input, I, for the damper is constant and equal to 2.5A for the results shown in Fig. 4. Good agreement between the MNS model and the test results is evident in Fig. 4. Table 2 presents a comparison of the normalized RMS error (Gavin 2001) for the MNS, Bouc-Wen, and hyperbolic-tangent damper models for two cases involving a constant current input of I=0.0A and 2.5A. For the case with I=0.0A the displacement history is based on Gaussian white noise with a bandwidth of 2Hz. As can be seen in Table 2, the MNS model shows better agreement with the test data than the other two models, particularly for the case of I=0.0A which involves larger velocities.

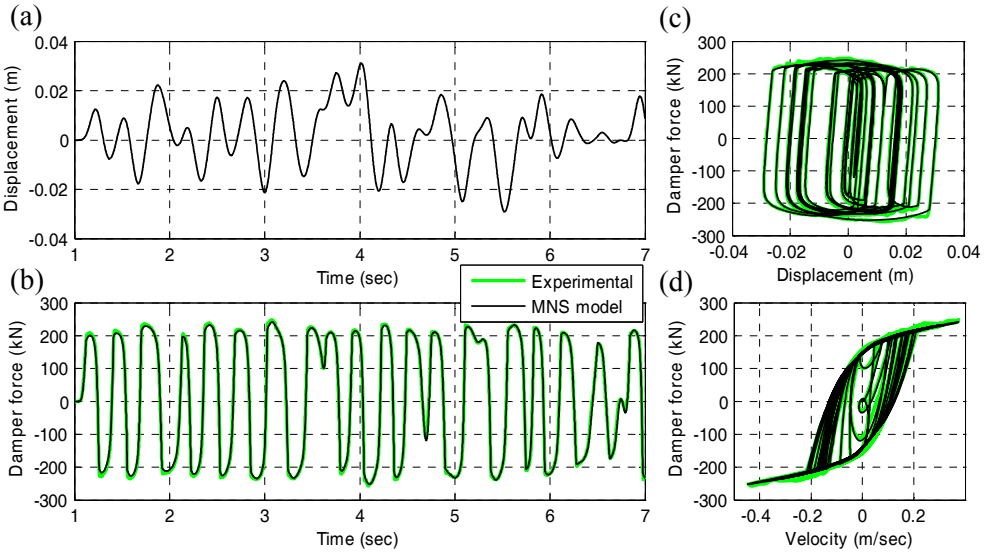

Figure 4. Comparison of predicted damper force by MNS model with experimental data (I=2.5A): (a) time history of input displacement; (b) time history of damper force; (c) force-displacement relationship; (d) force-velocity relationship.

Table 2. Comparison of normalized RMS error of MR damper models with band-limited Gaussian white noise

Damper Current I (Amps)	Gaussian white noise (displacement input)			Normalized RMS error		
	Max. disp. (m)	Max. velocity (m/s)	Bandwidth (Hz)	Bouc-Wen model	Hyperbolic tangent model	MNS model
0.0	0.050	0.452	2.0	0.1291	0.0992	0.0688
2.5	0.030	0.445	4.0	0.0420	0.0409	0.0370

Dynamics of MR Damper Associated with Variable Current

Dynamics of Current Driver (PWM Servo-Amplifier)

Due to the inductance of the electro-magnetic coil that generates the magnetic field in the damper, the current within the electro-magnetic circuit changes slowly if a voltage driven power supply is used (Yang et al. 2002). Yang presented a governing differential equation for the

electro-magnetic circuit based on the duty cycle of a PWM servo-amplifier and PI controller (Yang 2001). In this paper the same governing equation is used, from which a transfer function *G(s)* between the current output to the damper and current command signal for the current driver is derived:

$$G(s) = \frac{235s + 44522}{s^2 + 302s + 44522} \tag{8}$$

Dynamics of Electromagnetism

As noted previously, semi-active control algorithms have been develop for MR dampers. These control laws involve a variable current command to the damper. To understand the dynamics of an MR damper, it is necessary to investigate the dynamic behavior of the magnetic field in the damper associated with variable current. When the current changes inside the electromagnetic coil, a magnetic flux that is proportional to the current in the coil is generated. The magnetic flux induces eddy currents in the material around the coil (e.g., the piston head, cylinder housing), which opposes the magnetic flux generated by the coil according to Lenz's law. This results in the development of a time delay in the MR damper force under a variable current input (Takesue et al. 2004). The hysteresis of the magnetization of the MR damper fluid makes it difficult to predict the damper force, for the piston head and cylinder housing around the coil can develop a residual magnetic field after the applied magnetic field has been removed. This nonlinear hysteretic behavior not only can affect the induction of eddy currents, but it can also disturb the formation of the total magnetic field and the damper force. Therefore, the use of a first order filter (Spencer et al. 1997) for the description of the dynamics of a MR damper may not be sufficient to explain the complex behavior of an MR damper under a variable current input. To obtain a better prediction of the damper force under a variable current, this paper proposes a model based on the following nonlinear differential equation to relate the coil current to an equivalent static current:

$$\dot{I}_{eq} = \alpha(\dot{I}_r)(I - I_{eq}) \tag{9}$$

The function $\alpha()$ is determined from the Eq. (10) and (11).

$$\alpha(\dot{I}_r) = \begin{cases} a^+\dot{I}_r + \alpha_1 & \text{if } \dot{I}_r \geq 0 \\ a^-\dot{I}_r + \alpha_1 & \text{if } \dot{I}_r < 0 \end{cases} \tag{10}$$

$$\dot{I}_r = \alpha_0(I - I_r) \tag{11}$$

where, α_0, α_1, a^+ and a^- are constants which are obtained by utilizing nonlinear optimization theory to minimize the error between the predicted and experimental response of the damper force. I is a current in the coil, which is generated by the current driver. I_{eq} is an equivalent static current that can generate the same magnetic flux as the resultant magnetic flux at time t created by I, the eddy currents, residual magnetic fields, and other phenomena that affect the formation of the magnetic flux.

Fig. 5 shows the block diagram for this model. With I_{eq} obtained from the solution to Eq. 9, the parameter sets in Table 1 can be interpolated or directly used under variable current inputs

to specify the damper parameters for the model which enables the damper force to be calculated using the MNS model.

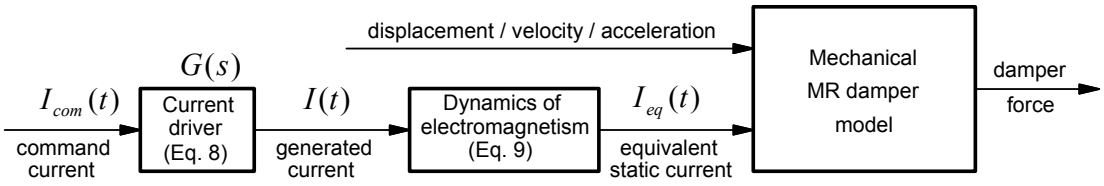

Figure 5. Block diagram for MR damper model under variable current

To assess the model, tests with variable displacement and current were performed, where the variation in current simulated that from the clipped optimal controller algorithm with a maximum current of 2.5A. Fig. 6 (a) and (b) show the pre-defined displacement and current time histories for the MR damper. The experimental response and MNS model prediction of the MR damper are shown in Fig. 6 (c) through (e). The values for the parameters for Eq. 9, 10 and 11 are: $\alpha_0 = 24.96$, $\alpha_1 = 3.57$, $a^+ = 0.31$, $a^- = -0.30$. As can be observed in Fig. 6, the MNS model can accurately predict the response of the MR damper under variable current.

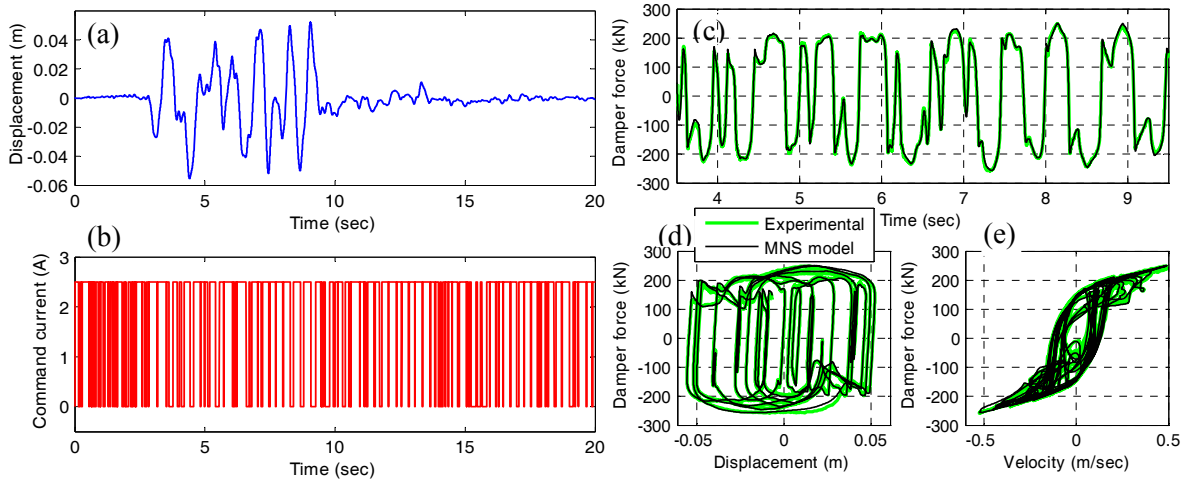

Figure 6. Response of large-scale MR damper under variable current: (a) time history of input displacement; (b) time history of input current; (c) time history of damper force; (d) force-displacement relationship; (e) force-velocity relationship.

Summary and Conclusions

A newly developed formulation was presented for the prediction of the dynamic behavior of large-scale MR dampers. The formulation consists of the Maxwell Nonlinear Slider model and an equivalent static current model to account for the effects caused by a variable input current. In the MNS model, the pre-yield and post-yield behaviors of an MR damper are independently described. This simplifies the identification of the model parameters from characterization tests. The MNS model utilizes the Hershel-Bulkley model to describe the post-yield behavior, thereby enabling the property of a non-Newtonian fluid to be readily included in the MNS model and the effects of shear thinning and thickening behavior of the MR fluid to be accounted for. To account for the time lag response of the MR damper force that occurs under with a variable

current input, a model based on a nonlinear differential equation was presented. Predictions made by the MNS model under constant and variable current inputs show good agreement with experimental results. Further studies of the dynamics of MR dampers needs to be conducted in order to evaluate and calibrate the formulation over a wider range of variable current inputs, and frequencies and amplitudes in the displacement history than those presented in this paper.

Acknowledgements

This paper is based upon work supported by grants from the Pennsylvania Department of Community and Economic Development through the Pennsylvania Infrastructure Technology Alliance, and by the National Science Foundation under Grant No. CMS-0402490 within the George E. Brown, Jr. Network for Earthquake Engineering Simulation Consortium Operation. The MR fluid dampers were provided by Dr. Richard Christenson at University of Connecticut. The authors appreciate his support.

References

Bass, B. J., and Christenson, R. E., 2007. System identification of a 200 kN, magneto-rheological fluid damper for structural control in large-scale smart structures, *Proc., Amer. Control Conf.*, NY, NY..

Butz, T and Von Stryk, O., 2002. Modelling and simulation of electro- and magneto-rheological fluid dampers, *ZAMM - Journal of Applied Mathematics and Mechanics* 82, 3-20.

Carlson, J. D., and Spencer, B. F., Jr., 1996. Magneto-rheological fluid dampers for semi-active seismic control, *Proc., 3rd Int. Conf. on Motion and Vibration Control* 3, Chiba, Japan, 35–40.

Dyke, S.J., Spencer Jr., B.F., Sain, M.K. and Carlson, J.D., 1996. Modeling and control of magneto-rheological dampers for seismic response reduction, *Smart Materials and Structures* 5, 565-575.

Gavin, H.P., 2001, Multi-duct ER dampers, *Jrnl of Intelligent Material Sys and Structures* 12, 353-366.

Herschel, W.H. and Bulkley, R., 1926. Konsistenzmessungen von Gummi-Benzollösungen*, Kolloid Zeitschrift* 39, 291–300.

Jansen, L.M. and Dyke, S.J., 2000. Semi-active control strategies for MR dampers: comparison study, *Journal of Engineering Mechanic*s 126(8), 795-803.

Kennedy, J. and Eberhart, R. C., 1995. Particle swarm optimization, *IEEE Int. Conf. on Neural. Networks (Perth)* 4, 1942–1949.

Ribakov, Y. and Gluck, J., 2002. Selective controlled base isolation system with magneto-rheological dampers, *Earthquake Engineering and Structural Dynamics* 31, 1301-1324.

Schurter, K. C. and Roschke, P. N., 2001. Neuro-fuzzy control of structures using acceleration feedback, *Smart Materials and Structures* 10, 770-779.

Sodeyama, H., Suzuki, K. and Sunakoda, K., 2004. Development of large capacity semi-active seismic damper using magneto-rheological fluid, *Journal of Pressure Vessel Technology* 126, 105-109.

Spencer, B. F., Dyke, S. J., Sain, M. K. and Carlson, J. D., 1997. Phenomenological model for magneto-rheological dampers, *Journal of Engineering Mechanics* 123(3), 230-238.

Takesue, N., Furusho, J. and Kiyota, Y., 2004. Fast response MR-fluid actuator, *JSME International Journal Series C* 47(3), 783-791.

Yang, G., 2001. Large-Scale Magneto-rheological fluid damper for vibration mitigation: modeling, testing and control, *Ph.D Dissertation*, Department of Civil Engineering and Geological Sciences, University of Notre Dame, Notre Dame, Indiana.

Yang, G., Spencer Jr., B. F., Carlson, J. D., Sain, M. K., 2002. Large-scale MR fluid dampers: modeling and dynamic performance considerations, *Engineering Structures* 24, 309-323.